# *Arabidopsis* gp91$^{phox}$ homologues *AtrbohD* and *AtrbohF* are required for accumulation of reactive oxygen intermediates in the plant defense response

**Miguel Angel Torres\*, Jeffery L. Dangl\*†‡, and Jonathan D. G. Jones§**

*Department of Biology and †Curriculum in Genetics and Molecular Biology, CB 3280, 108 Coker Hall, University of North Carolina, Chapel Hill, NC 27599-3280; and §The Sainsbury Laboratory, John Innes Centre, Colney, Norwich NR4 7UH, United Kingdom

Reactive oxygen intermediates (ROI) are strongly associated with plant defense responses. The origin of these ROI has been controversial. *Arabidopsis* respiratory burst oxidase homologues (*rboh* genes) have been proposed to play a role in ROI generation. We analyzed lines carrying *dSpm* insertions in the highly expressed *AtrbohD* and *AtrbohF* genes. Both are required for full ROI production observed during incompatible interactions with the bacterial pathogen *Pseudomonas syringae* pv. tomato DC3000(*avrRpm1*) and the oomycete parasite *Peronospora parasitica*. We also observed reduced cell death, visualized by trypan blue stain and reduced electrolyte leakage, in the *Atrboh* mutants after DC3000(*avrRpm1*) inoculation. However, enhanced cell death is observed after infection of mutant lines with *P. parasitica*. Paradoxically, although *atrbohD* mutation eliminated the majority of total ROI production, *atrbohF* mutation exhibited the strongest effect on cell death.

**E**arly production of reactive oxygen intermediates (ROI) is a hallmark of the plant defense response. Many studies document the detection of $O_2^-$ and/or its dismutation product, $H_2O_2$, during incompatible interactions between resistant plants and avirulent pathogens (1–4). During the defense response, ROI can inhibit the pathogen by strengthening cell walls via oxidative cross-linking of cell-wall glycoproteins (5) or by directly killing the pathogen (3). ROI also could act as signals to induce further defenses (6–9), including the initiation of the hypersensitive response (HR). Nitric oxide (NO), another reactive molecule that works synergistically with ROI in driving mammalian cell death in macrophages (10), also has emerged as an important mediator of plant defense response and cell death signaling in plants (11, 12).

The likely source of ROI is an NADPH oxidase, originally postulated to be membrane-bound and to use molecular oxygen to make superoxide, based partly on inhibition studies using diphenylene iodonium (1). This NADPH oxidase is thought to be at least partially similar to the one present in the mammalian phagocytes (13, 14). In activated macrophages, the respiratory burst NADPH oxidase (RBO) is responsible for generation ROI (14). Mutations in *gp91$^{phox}$*, encoding the catalytic subunit of the NADPH oxidase, result in chronic granulomatous disease, an immunological disorder in which macrophages are unable to stop the spread of infection (15). Several plant *rboh* genes, homologous to *gp91$^{phox}$*, were identified, although they carry a 300-aa N-terminal extension compared with the mammalian proteins (16–19). Rac homologues in rice have been implicated in pathogen-induced cell death occurring in this plant (20), and Rac is required for assembly of an active respiratory burst NADPH oxidase in animals (14). However, no homologues to the *p47* or *p67* regulators of the mammalian NADPH oxidase were found in the *Arabidopsis* genome (21). These findings suggest that a superoxide-generating NADPH oxidase does exist in plants, although the plant NADPH oxidase is most likely regulated differently than the one present in mammalian macrophages. Alternative mechanisms of ROI production in plants

also have been proposed invoking cell-wall-bound peroxidases as the main ROI source (22, 23).

Using a *dSpm* insertion mutagenesis system (24), we isolated mutants in eight *Atrboh* genes. We demonstrate that *atrbohD* and *atrbohF* mutations largely eliminate ROI accumulation during disease-resistance reactions of *Arabidopsis* to avirulent *Pseudomonas syringae* and *Peronospora parasitica* (*Pp*). Hence, an NADPH oxidase is responsible for ROI accumulation during some defense responses in *Arabidopsis*.

## Materials and Methods

**Identification of the *Atrboh* Mutants.** Insertions in *AtrbohD* and *F* were identified through a PCR screen on genomic DNA extracted from pools of Col-0 plants containing *dSpm* transposon insertions (24). Primers used include dSpm11 and dSpm1 from the transposon (24) and specific primers from each *Atrboh* gene: D122 (ATGAAAATGAGACGAGGCAATTC), D92b (GGATACTGATCATAGGCGTGGCTCCA), F171 (CTTCCGATATCCTTCAACCAACTC), and F172 (GAGATTGCCTTTATACTATAAGTG).

Insertions in each gene were confirmed by sequencing PCR products spanning the insertion. All of the lines identified contained a single transposon and were derived from gluforinate ammonium (BASTA)-resistant heterozygote parents. Plants were grown in a chamber under a 9-h photoperiod, 24°C day and 20°C night temperatures, 60% relative humidity, and 250 $\mu$einsteins/m²/s.

**Test with Pathogens.** Bacterial strains used in this study were *P. syringae* pv. tomato (*Pst*) DC3000, DC3000(*avrRpm1*), and DC3000(*avrRpt2*). Four-week-old plants were inoculated in a standard manner (25). *atrbohD/F* plants that did not display necrotic lesions were selected before infection. Various *Pp* isolates, Emco5, Cala2, Emwa1, Noco2, or Ahco1, were sprayed on 11-day-old seedlings (26).

**Cell Death Measurements.** Trypan blue stain, used to visualize dying cells, was performed as described (27). The protocol for electrolyte leakage was adapted from Dellagi *et al.* (28). Four-week-old plants were injected with bacteria in 10 mM MgCl₂. Ten minutes after injection, 7.5-mm-diameter leaf discs were collected from the injected area and washed extensively with water for 50 min, and

---

**PLANT BIOLOGY**

then four discs were placed in a tube with 6 ml of water. Conductivity measurements (3–4 replicates for each treatment) were taken from the tubes over time by using an Orion (Boston) conductivity meter, model 130. The units of this measurement are $\mu S/cm$, where cm refers to the distance between electrodes. No increase in the conductivity was observed when plants were injected with $MgCl_2$ or virulent DC3000.

**Detection of ROI.** To visualize $H_2O_2$ *in situ*, 3,3′-diaminobenzidine (DAB) staining was performed on *Arabidopsis* seedlings sprayed with *Pp* spores as described (29). For bacterial experiments with DC3000(*avrRPm1*), leaves were collected 2 h after injection of the bacteria and vacuum-infiltrated with the DAB solution. Leaves then were placed in a plastic box under high humidity until brown precipitate was observed (5–6 h) and then fixed with a solution of 3:1:1 ethanol/lactic acid/glycerol. Catalase effectively eliminated the DAB stain. Application of glucose/glucose oxidase or $H_2O_2$ directly to leaves was used to verify that *atrboh* mutants are not impaired in the detection of ROI by this method. Quantification of the staining was performed with QUANTISCAN (Biosoft, Milltown, NJ), using 20 leaves similar to the ones presented in Fig. 2*A*, coming from two different experiments. The index of staining was calculated for each leaf injected as the average of the index of brown pixels measured in three points inside the injected area minus the average of three points in the opposite side of each leaf.

## Results

**Identification of Mutants in *AtrbohD* and *AtrbohF*.** *AtrbohD* and *AtrbohF* are the highest expressed *Atrboh* genes in leaves (18), the tissue infected by our test pathogens. Thus, we focused on mutants in these two genes to test the role of NADPH oxidase in ROI production. We identified *atrbohD* and *atrbohF* mutants through PCR-based screening of pooled DNA from *Arabidopsis* plants containing random *dSpm* transposons in their genome (24). Insertion D3 is located in the fifth exon of *AtrbohD* after codon P535 (after nucleotide T1605 from the ATG). Insertions F3 and F4 are located in the first exon of *AtrbohF*, in codon Q177 (after nucleotide A530) and I221 (after nucleotide A661). F5 is in the second intron of *AtrbohF*, 11 nt downstream of the splice donor. Lines homozygous for the respective insertions were identified by PCR after gluforinate ammonium selection in the next generation. All three independent *atrbohF* mutant lines gave similar phenotypes with pathogens; therefore, we used only insertion F3 for these studies.

To verify that these mutant lines are null alleles, we performed RNA gel blot analyses and reverse transcription–PCR with specific primers on total RNA extracted from 10-day-old seedlings. These analyses revealed no normal full-length transcript, some aberrant transcripts, and chimeras between the transposon and the *atrboh* mRNA that presumably would give rise to nonfunctional proteins. *atrbohD* and *atrbohF* mutants are morphologically normal, although they look slightly smaller than wild type (wt) (Fig. 1*B*). This phenotype is enhanced in the *atrbohD/F* double mutant. Four-week-old *atrbohD/F* plants display some necrotic lesions and callose deposition (Fig. 1 *C* and *D*). Some of these plants stop growing and die before setting seeds. Importantly, in the experiments described below, we used morphologically normal plants at ages well before this phenotype developed.

**Reduction of ROI Accumulation and Diminished Cell Death Symptoms in the *atrboh* Mutants After Inoculation with Avirulent *P. syringae*.** We examined the contribution of *AtrbohD* and *AtrbohF* to ROI production during responses to pathogenic bacteria. DAB polymerizes on contact with $H_2O_2$ in a reaction requiring peroxidase. Thus, $H_2O_2$ is visualized *in situ* as a reddish-brown precipitate (29). We observed a strong, brown precipitate in wt plants starting 3–4 h postinjection of the avirulent strain DC3000(*avrRpm1*) (Fig. 2 *A* and *C*), in accordance with previous observations of *RPM1* func-
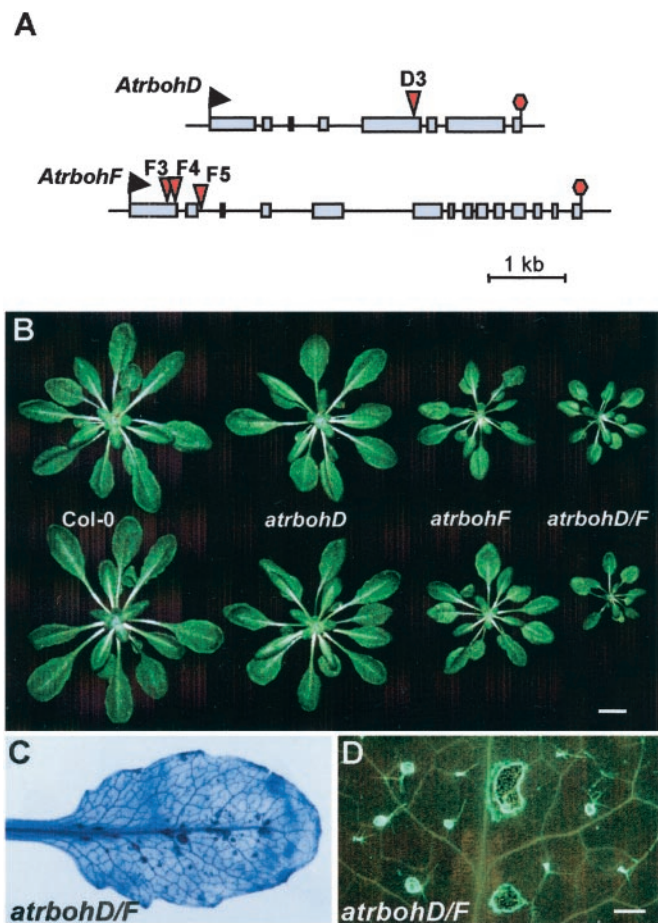


**Fig. 1.** *Arabidopsis atrbohD* and *atrbohF* mutants. (*A*) Schematic representation of the transposon insertions in the *Atrboh D* and *F* genes. Boxes represent the exons of the genes, and red triangles mark the *dSpm* transposon insertions. (*B*) Representative 4-week-old rosettes. (*C*) Trypan blue staining of an *atrbohD/F* double mutant leaf, displaying spontaneous necrosis. (*D*) Detail of an *atrbohD/F* leaf stained with aniline blue to show callose deposition. Note that infection experiments are performed on young plants that do not exhibit ectopic cell death. [Bar = 1 cm (*B*) and 1 mm (*D*).]

tion, by using $CeCl_3$ staining (30). No stain was observed after injection of virulent DC3000 or $MgCl_2$ (data not shown).

We conducted similar analyses with the *atrbohD*, *atrbohF*, and *atrbohD/F* double mutants. Although there was no change in DAB staining intensity in the *atrbohF* mutant compared with wt, staining is greatly reduced in the mutant *atrbohD* and in the double mutant *atrbohD/F* (Fig. 2 *A* and *C*). Similar results were obtained with DC3000(*avrRpt2*) (which produces a delayed HR compared with DC3000(*avrRpm1*); data not shown). Quantification of the DAB stain demonstrates that *atrbohD* and *atrbohD/F* double mutants display levels of DAB precipitate comparable to control plants inoculated with virulent DC3000 or $MgCl_2$ (Fig. 2*B*). Trypan blue staining performed in additional leaves from the same experiment indicates that the DAB-staining procedure does not interfere with the progression of the HR (see below). Thus, *Arabidopsis AtrbohD* is required for most of the ROI observed after inoculation with avirulent *Pst*, whereas *AtrbohF* contributes little to this oxidative burst.

We wanted to study the requirement of *Atrboh*-generated ROI for HR and disease resistance. Although ROI production is strongly correlated with the early defense response, temporally preceding either HR or cessation of pathogen growth (31), it is unclear whether the oxidative burst is required for HR and/or stopping
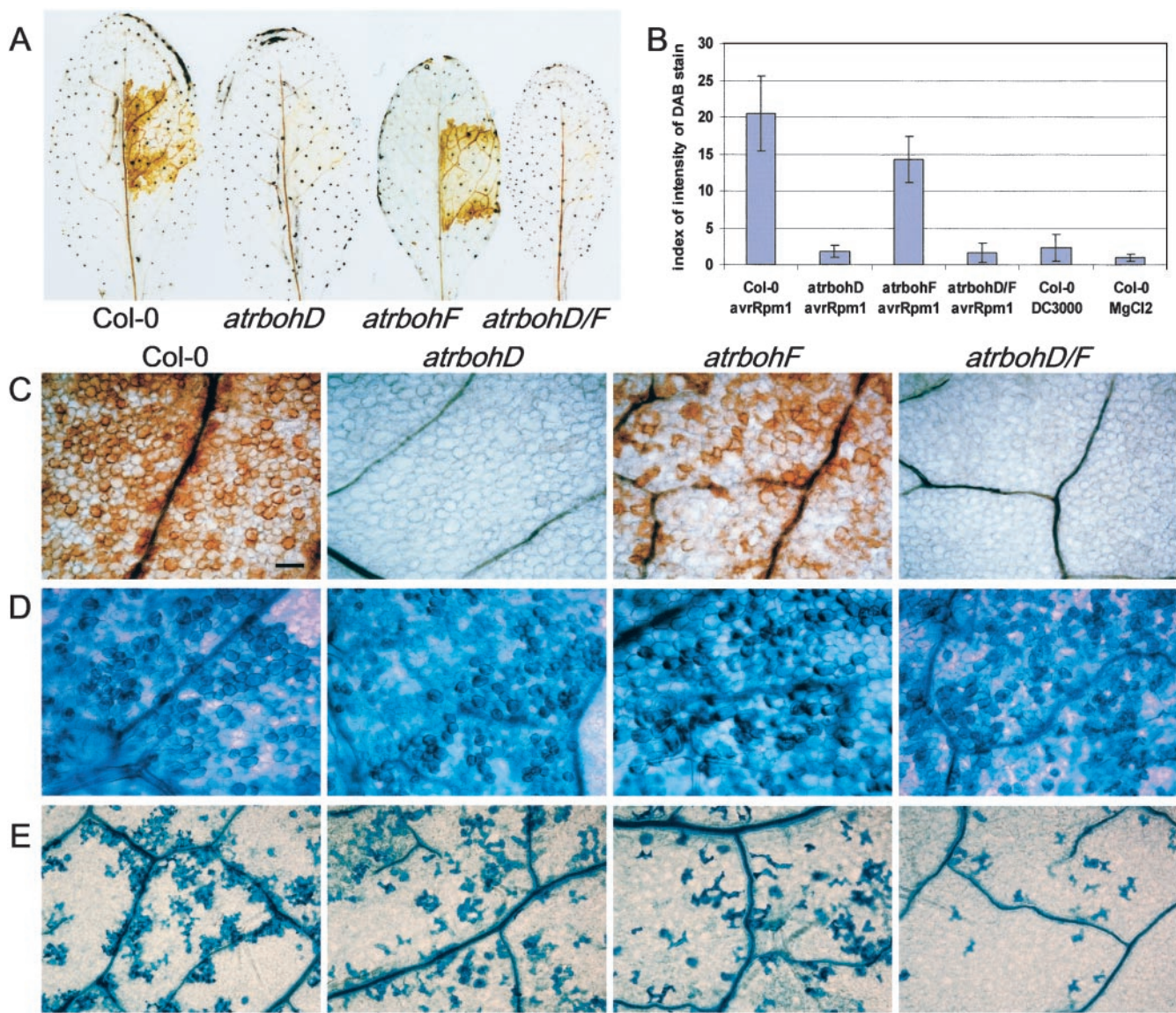
**Fig. 2.** Reduced ROI accumulation and cell death in the *atrboh* mutants after inoculation of avirulent bacteria. (*A*) *In situ* detection of peroxides by using DAB staining on wt Col-0 and *atrboh* mutant leaves 5 h postinoculation with DC3000(*avrRpm1*) at $2.5 \times 10^7$ cfu/ml. (*B*) Quantitative analysis of DAB on leaves 6 h postinoculation with DC3000(*avrRpm1*) at $2.5 \times 10^7$ cfu/ml, DC3000 (same inoculum concentration), or 10 mM MgCl$_2$. (Bars = SD.) (*C*) Detail of leaves stained with DAB 5 h postinoculation with DC3000(*avrRpm1*) at $2.5 \times 10^7$ cfu/ml. Genotypes are labeled at the top, left to right: Col-0, *atrbohD*, *atrbohF*, and *atrbohD/F*. (*D*) Detail of leaves stained with trypan blue 5 h postinoculation with DC3000(*avrRpm1*) at $2.5 \times 10^7$ cfu/ml. (*E*) Detail of leaves stained with trypan blue 12 h postinoculation with lower dose of DC3000(*avrRpm1*), $10^6$ cfu/ml. (Bar = 25 $\mu$m.) All images in *C–E* have the same magnification.

pathogen growth. Inoculation of avirulent DC3000(*avrRpm1*) or virulent DC3000 bacteria under conditions in which the former initiates a rapid hypersensitive reaction ($\approx 2.5 \times 10^7$ cfu/ml) showed no clear differences in trypan blue staining between wt and *atrboh* mutants (Fig. 2*D* and data not shown). However, the *atrboh* mutants displayed less trypan blue stain than the wt after injection of an inoculum ($10^6$ cfu/ml) of DC3000(*avrRpm1*) that more closely reflects natural infection pressure. In particular, the *atrbohD/F* double mutant displayed reduced localized cell death compared with Col-0 (Fig. 2*E*). Measurement of *in planta* growth of both avirulent and virulent bacterial strains revealed no significant differences between the wt and the *atrboh* mutants (data not shown).

We monitored electrolyte leakage to quantify cell death during the HR (28). Leaf discs excised from control wt leaves infiltrated with DC3000(*avrRpm1*) exhibited significantly increased ion leak-

age compared with MgCl$_2$ or DC3000 controls 4–6 h after injection (Fig. 3*A*). This corresponds to a time when leaves begin to exhibit macroscopic HR. The *atrbohD/F* double mutant displayed significantly lower ion leakage in repeated experiments (Fig. 3*A*). Mutations in *atrbohF* and *atrbohD* act redundantly in this assay. *atrbohF* mutants exhibit reproducibly greater diminution of ion leakage than *atrbohD* (Fig. 3*B*). Collectively, these data suggest that *AtrbohD* is responsible for most of the ROI produced in response to inoculation of avirulent *Pst*. Conversely, *AtrbohF* plays a key role in HR, particularly at low-dose inoculation. By contrast, ROI apparently are dispensable for mediating at least the *RPM1*-dependent signals that limit bacterial growth.

**Atrboh Genes Modulate the Response to *Pp* Emco5 Infection.** We evaluated whether the *atrboh* mutants have an effect on the resistance response against the oomycete parasite *Pp. Pp* isolate Emco5 is fully virulent on Col-0 cotyledons, but triggers resistance,
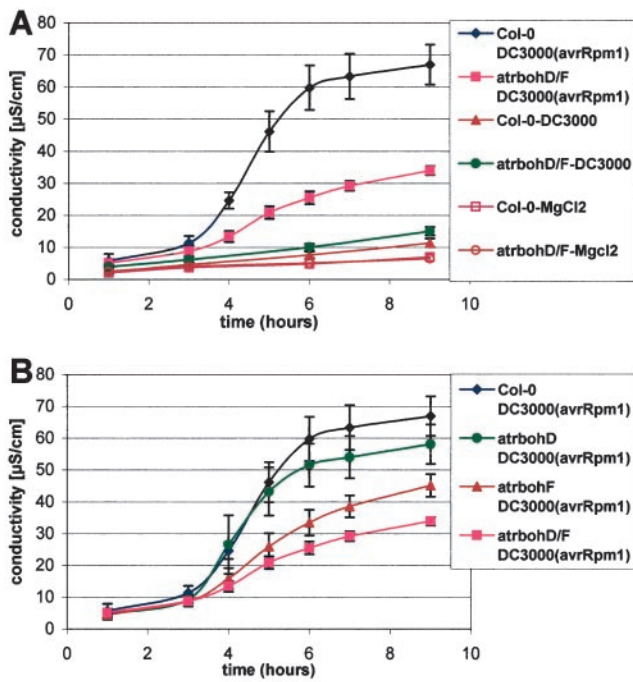
**Fig. 3.** Reduced electrolyte leakage in *atrboh* mutants after inoculation with avirulent bacteria. (*A*) Conductivity ($\mu$S/cm) of solution containing leaf discs from either wt Col-0 or *atrbohD/F* mutant inoculated with avirulent bacteria DC3000(*avrRpm1*) at $10^7$ cfu/ml, virulent bacteria DC3000 at $10^7$ cfu/ml, or 10 mM MgCl$_2$. (*B*) Detailed differences in conductivity between Col-0 and the *atrboh* mutants during the incompatible interaction DC3000(*avrRpm1*) at $10^7$ cfu/ml. Each value represents the mean and SD of three replicates (compatible interaction and MgCl$_2$) or four replicates (incompatible interactions) per experiment. The experiment was repeated three times with similar results.
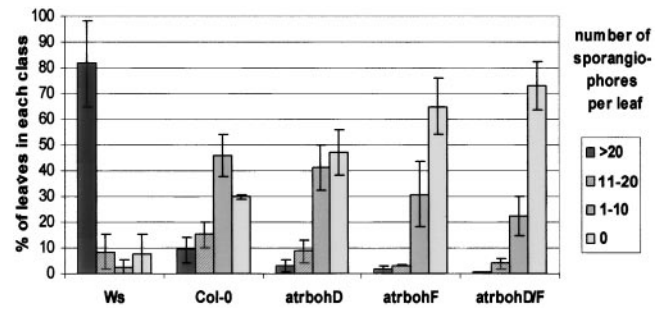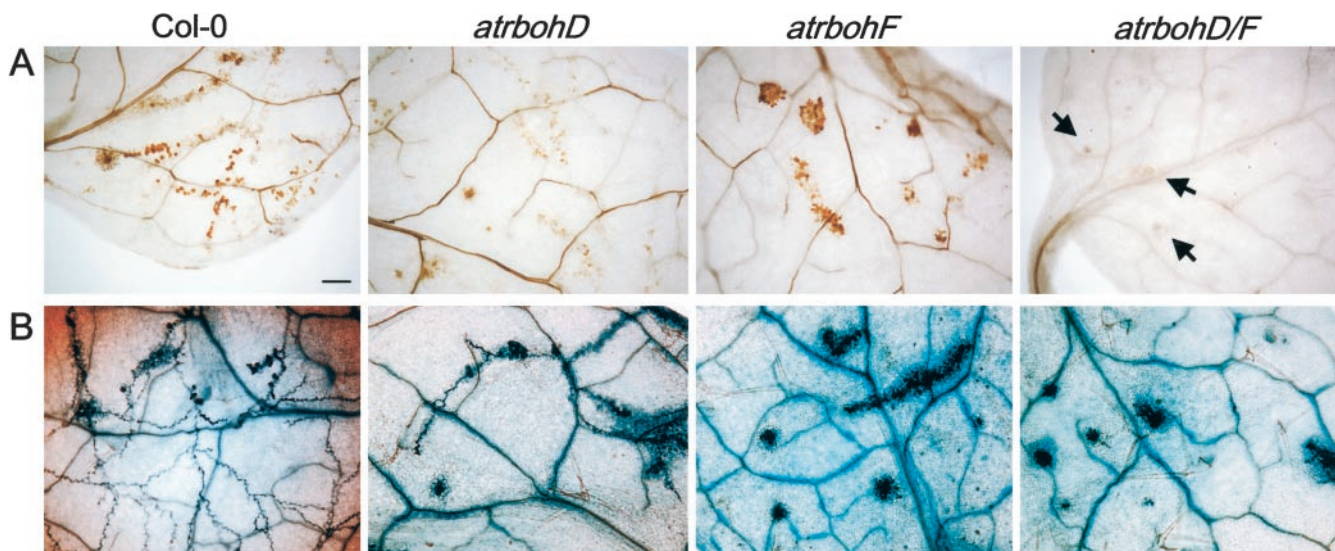


**Fig. 5.** Reduced sporangiophore formation in the *atrboh* mutants. The histogram represents the percentage of first leaves of seedlings (genotypes at bottom) that display >20, 11–20, 1–10, or 0 sporangiophores 7 days postinoculation with *Pp* isolate Emco5. The data are the mean and SD from three different experiments representing more than 200 total leaves evaluated for each genotype.

appearance of HR revealed by trypan blue staining (Fig. 4). Thus, this adult resistance is weaker than the resistance mediated by the majority of *R* genes directed against *Pp*, because the latter typically are associated with discrete HR.

Peroxide production, but not the typical trailing necrosis, triggered by *Pp* Emco5 is greatly reduced in *atrbohD* mutants (Fig. 4). Strikingly, both DAB staining and HR are enhanced, and focused into discrete HR lesions, in *atrbohF* plants (Fig. 4). Peroxide production is eliminated in the *atrbohD/F* double mutant but HR is also enhanced. The enhanced HR surrounds the emerging hyphae and prevents their growth in nearly all cases. This enhanced response also results in less sporangiophore formation in true leaves of the *atrbohF* and *atrbohD/F* double mutants compared with wt (Fig. 5). Consequently, at least in this interaction, assaying the weak adult *R* function directed toward *Pp* Emco5, *atrbohD*, and *atrbohF* results in separable phenotypes. The *atrbohD* mutation eliminates most of the peroxide produced, whereas *atrbohF* actually allows enhanced cell HR and improved resistance toward the parasite.

We also infected the *Atrboh* mutants with two additional avirulent isolates of *Pp*, Emwa1 and Cala2, that are recognized by the Col-0 *RPP4 and RPP2* genes, respectively. These interactions result in typical HR limited to a discrete group of cells (32). *atrbohD* and the *atrbohD/F* double mutants exhibited reduced peroxide produc-

conditioned by a single locus, in the emerging true leaves (J. M. McDowell, S. Williams, and J.L.D., unpublished data). This "adult resistance" is associated with HR trailing the growing hyphae (trailing necrosis). DAB stain reveals peroxide production in the wt around the growing Emco5 hyphae in a pattern that resembles the



**Fig. 4.** Reduced peroxide accumulation and enhanced cell death in the *atrboh* mutants after inoculation with *Pp* isolate Emco5. (*A*) DAB staining of leaves 3 days after inoculation with *Pp* isolate Emco5. Arrows indicate HR sites in *atrbohD/F*. (*B*) Trypan blue stain of leaves from the same experiment 3 days after inoculation with *Pp* isolate Emco5. The experiment was repeated four times; ≈10 leaves per genotype per experiment analyzed. (Bar = 50 $\mu$m for all.)

tion in these interactions (data not shown). However, depletion of ROI in these experiments had no effect on either cell death or resistance. Additionally, we observed no DAB staining and no effect on disease progression after infection with virulent *Pp* isolates Noco2 and Ahco1 in either the Col-0 or the *atrboh* mutants (data not shown). This demonstrates that our data are not a result of general induction of defense response.

## Discussion

We used reverse genetics in *Arabidopsis* to define functions for two *Atrboh* genes in the production of ROI during the defense response. We observed depletion of DAB staining, a standard marker of ROI accumulation, in these mutants after challenge with avirulent *Pst* or *Pp*. The *AtrbohD* gene is required for most of the ROI observed after inoculation with avirulent *Pst*, whereas *AtrbohF* makes a more limited contribution. In contrast, the *atrboh* mutants exhibit enhanced HR and less sporangiophore formation in response to the weakly avirulent *Pp* Emco5. Interestingly, although *atrbohF* exhibits minor diminution of ROI production, it expresses strongly enhanced cell death phenotypes. Finally, we demonstrate that the *atrbohD/F* double mutant exhibits even further reduced HR against *Pst* but enhances a weak resistance response against *Pp*. Thus, our most important findings are: (i) extracellular ROI production in *Arabidopsis* requires *Atrboh* function, (ii) *AtrbohD* and *AtrbohF* share functions in ROI generation but have separable functions in HR regulation, and (iii) *atrbohF* mutants have a limited effect on ROI production compared with *atrbohD* but a much greater effect on *Pp*-induced cell death.

We provide genetic evidence that *AtrbohD* and *AtrbohF*, encoding probable components of a plant NADPH oxidase, are responsible for the ROI produced in two widely used systems for the analysis of plant defense responses. Controversy regarding the origin of ROI in plant defense has existed since Doke (1) first documented the production of superoxide in potato tubers infected with *Phytophthora infestans*. Subsequent definition of similarities to the oxidative burst in mammalian macrophages suggested that an NADPH oxidase was responsible for this ROI production (13). However, $H_2O_2$, and not superoxide, is the ROI detected in most plant–pathogen interactions (2, 3). These data suggested either that $H_2O_2$ is the proximal burst product or that rapid dismutation converts superoxide to $H_2O_2$. Other studies demonstrated in several systems that superoxide is, in fact, the proximal burst product and suggested that $H_2O_2$ is not the key signal for HR or defense-response control in these systems (33, 34). Sagi and Fluhr (35), using a novel activity gel assay, recently confirmed that a putative plant plasma membrane NADPH oxidase can produce superoxide.

Cell wall-bound peroxidases were proposed as an alternate source for ROI–$H_2O_2$ generation (36). Induced gene expression and enzymatic activity concomitant with the burst also implicated oxalate oxidases in ROI production during powdery mildew–barley interactions (23). However, these studies are based on correlations derived from gene expression and protein accumulation. Additionally, some of these conclusions rest on pharmacological studies that require careful interpretation and specificity controls. There is, to date, no direct genetic evidence supporting peroxidase or oxalate oxidase as sources of the ROI produced after infection.

Although $H_2O_2$ is the main ROI detected in many plant pathogen systems and cell culture systems (2, 3), our demonstration that an NADPH oxidase subunit is required for ROI production confirms Doke's original suggestion that $O_2^-$ is the first ROI produced (at least in interactions with avirulent *Pst* or *Pp*). Thus, our results support previous findings identifying $O_2^-$ as the key regulatory molecule (31, 33, 37). However, we failed to detect $O_2^-$ by nitroblue tetrazolium stain or cytochrome *c* reduction after infection (data not shown). In fact, we observed less nitroblue tetrazolium precipitate directly in leaf panels injected with avirulent bacteria than in the surrounding areas (data not shown). This might be a result of rapid superoxide dismutase activity that increases after pathogen

inoculation (38, 39). This suggestion begs the question of how membrane-impermeable $O_2^-$ is dismutated in the absence of demonstrable extracellular superoxide dismutase activity. Alternatively, the $O_2^-$ is dismutated rapidly in a superoxide dismutase-independent, nonenzymatic manner. Its rate of nonenzymatic dismutation is close to $10^5$ $M^{-1}s^{-1}$, whereas its reaction rate with nitroblue tetrazolium is $6 \times 10^4$ $M^{-1}s^{-1}$ (40).

Our analysis of the *atrbohD* and *atrbohF* mutants strongly suggests that these genes act together to produce ROI (*AtrbohD*) and to control cell death (*AtrbohF*) in response to avirulent *Pst* DC3000(*avrRpm1*) because the double mutant HR reduction phenotype is stronger than *atrbohF*. However, HR appears not to be required for limiting bacterial growth. Other studies indicated separation between cell death and resistance to pathogens. For example, *dnd1* mutant (defense, no death) displays normal gene for gene resistance to bacterial pathogens although the HR appears inhibited (41).

The HR provoked by Pst DC3000(*avrRpm1*) is not suppressed completely in the *atrboh* mutants. Both trypan blue stain and electrolytic leakage measurements indicate residual HR in the *atrbohD/F* double mutant that might be explained by residual ROI below our limit of detection (Fig. 2 *A–C*). Alternatively, other mechanisms may contribute to the cell death induced during interaction with avirulent bacteria. Trypan blue stain after inoculation of $10^6$ cfu/ml DC3000(*avrRpm1*) identifies localized lesions in the *atrbohD/F* double mutant, compared with more spreading staining in the wt at each infection point (Fig. 2*E*). Therefore, the proximally produced ROI may act not as the initial trigger for HR in the directly infected cells but, rather, as a local signal for HR in nearby cells.

ROI may play a role in the establishment of systemic acquired resistance (SAR), a defense system that acts in distal parts of an infected plant (42). Salicylic acid (SA) is required for this establishment of SAR, because SAR is compromised in *nahG* plants that have reduced SA (43, 44). However, SA itself is not the translocated signal that mediates SAR (45, 46). SA and ROI metabolism are interconnected because ROI accumulation is potentiated by very small doses of SA (6, 47) and ROI induce SA accumulation (48). $H_2O_2$ has been proposed as a systemic signal (9). However, Dorey *et al.* (49) indicate that $H_2O_2$ is neither necessary nor sufficient to drive the expression of defense markers in areas surrounding infection sites. We induced SAR by inoculation of DC3000(*avrRpt2*) and assayed distal leaves for both protection against virulent *Pp* isolates and expression of the SAR-related gene *PR-1*. None of the *atrboh* mutants were compromised in their ability to mount an SAR response (data not shown). Thus, even in plants devoid of an oxidative burst, SAR still can be induced.

Surprisingly, we identified two different roles in HR control for *Atrboh*-generated ROI. Although the *atrboh* mutants, especially the *atrbohD/F* double mutant, display less HR after inoculation with avirulent *Pst*, they exhibit enhanced HR after inoculation with *Pp* Emco5. This unexpected phenotype was revealed only when we assayed the function of a weak *R* gene (J. M. McDowell, S. Williams, and J.L.D., unpublished data). This weak recognition does not completely block sporulation. The *atrboh* mutants display stronger cell death around the growing hyphae that prevents sporulation. Note that this is not simply enhancement of basal defense because it does not occur in response to infection with either of two virulent *Pp* isolates. We suggest that HR may have a clear mechanistic relation to resistance in interaction with the *Pp*, as has been demonstrated for the interaction of powdery mildew and barley (50). Our failure to define an effect of *atrboh* mutants on stronger *R*-mediated HR responses could reflect the fact that, despite ROI depletion, sufficient *R* signaling was generated. This concept is in line with findings of Bendahmane *et al.* (51), demonstrating that HR occurrence and magnitude can be correlated directly to R and Avr protein levels.

How can suppression of *atrboh*-dependent ROI lead to enhanced cell death? One possible scenario is provided by Delledonne *et al.* (38). In mammalian phagocytes, superoxide reacts with NO generating peroxynitrite ($ONOO^-$), a very reactive molecule with many biological targets (52). Delledonne *et al.* (38) suggest that the bacterial-induced HR in soybean suspension-cultured cells requires a fine poise between ROI and NO. However, HR does not appear to be mediated directly by $ONOO^-$. NO and $O_2^-$ accumulate independently after pathogen recognition (12). When the two are in balance, $ONOO^-$ can be formed, which is, in fact, not lethal in plants (38). However, increased superoxide dismutase activity, or spontaneous dismutation, drives $O_2^-$ into $H_2O_2$, potentially forcing an $NO/O_2^-$ imbalance. As a consequence, free NO accumulates and, together with $H_2O_2$, initiates HR.

Thus, NO and $H_2O_2$ are the elements directly involved in inducing cell death. Yet, $O_2^-$ is the proximal ROI produced, and its levels and rates of conversion to either $ONOO^-$ or $H_2O_2$ determine the outcome. In agreement with these studies, the effect of NO in potato as a protectant against ROI-mediated cytotoxic processes indicates a fine balance between NO/ROI to produce cell death and a role of $ONOO^-$ as a harmless sink for these reactive species (53). NO is a likely mediator of HR, but its activity is contingent on relative ROI levels. Reduction of ROI levels in the *atrboh* mutants would imply reduction of both positive ($H_2O_2$) and negative signals ($O_2^-$, in its role as a scavenger of NO) for the HR. The alteration of the fine balance between ROI and NO may explain the opposite effect observed between *Pst* and *Pp* responses. Alteration in the levels of NO also may be the origin of the spontaneous necrosis displayed by old *atrbohD/F* plants (Fig. 1*B*).

## Concluding Remarks

The identification of the insertion mutations in *AtrbohD* and *F* enabled a stringent test of their role in plant defense. We demonstrate that these proteins are responsible for the ROI production observed in some interactions with avirulent pathogens. The *AtrbohD* contribution to ROI production in leaves is greater than *AtrbohF*. However, *atrbohF* mutants display a stronger effect on cell death, which indicates a qualitative (spacial or temporal) difference in the ROI produced by each *Atrboh*. Depletion of ROI production in these lines has opposite effects on cell death: HR is reduced during interaction with DC3000(*avrRpm1*) and enhanced after *Pp* Emco5. This suggests a different role for ROI in cell death signaling in resistance to these pathogens. We propose that the enhanced cell death phenotype that these mutants display in the Emco5 interaction may be produced through an effect of this ROI depletion on the levels of other signaling components of the defense–cell death response, particularly NO.

1. Doke, N. (1983) *Physiol. Plant Pathol.* **23,** 359–367.
2. Apostol, I., Heinstein, P. F. & Low, P. S. (1989) *Plant Physiol.* **99,** 109–116.
3. Levine, A., Tenhaken, R., Dixon, R. & Lamb, C. J. (1994) *Cell* **79,** 583–593.
4. Nürnberger, T., Nennstiel, D., Jabs, T., Sacks, W. R., Hahlbrock, K. & Scheel, D. (1994) *Cell* **78,** 449–460.
5. Bradley, D., Kjellbom, P. & Lamb, C. (1992) *Cell* **70,** 21–30.
6. Shirasu, K., Nakajima, H., Rajasekhar, V. K., Dixon, R. A. & Lamb, C. J. (1997) *Plant Cell* **9,** 261–270.
7. Hammond-Kosack, K. E. & Jones, J. D. G. (1996) *Plant Cell* **8,** 1773–1791.
8. Lamb, C. & Dixon, R. A. (1997) *Annu. Rev. Physiol. Plant Mol. Biol.* **48,** 251–275.
9. Alvarez, M. E., Pennell, R. I., Meijer, P.-J., Ishikawa, A., Dixon, R. A. & Lamb, C. (1998) *Cell* **92,** 773–784.
10. Schmidt, H. H. H. & Walter, U. (1994) *Cell* **78,** 919–925.
11. Delledonne, M., Xia, Y., Dixon, R. A. & Lamb, C. J. (1998) *Nature (London)* **394,** 585–588.
12. Durner, J., Wendehenne, D. & Klessig, D. F. (1998) *Proc. Natl. Acad. Sci. USA* **95,** 10328–10333.
13. Low, P. S. & Merida, J. R. (1996) *Physiol. Plant.* **96,** 533–542.
14. Segal, A. W. & Abo, A. (1993) *Trends Biochem. Sci.* **18,** 48–52.
15. Roos, D., Deboer, M., Kuribayashi, F., Meischl, C., Weening, R. S., Segal, A. W., Ahlin, A., Nemet, K., Hossle, J. P., Bernatowska-Matuszkiewicz, E., *et al.* (1996) *Blood* **87,** 1663–1681.
16. Groom, Q. J., Torres, M. A., Fordham-Skelton, A. P., Hammond-Kosack, K. E., Robinson, N. J. & Jones, J. D. G. (1996) *Plant J.* **10,** 515–522.
17. Keller, T., Damude, H. G., Werner, D., Doerner, P., Dixon, R. A. & Lamb, C. (1998) *Plant Cell* **10,** 255–266.
18. Torres, M.-A., Onouchi, H., Hamada, S., Machida, C., Hammond-Kosack, K. E. & Jones, J. D. G. (1998) *Plant J.* **14,** 365–373.
19. Amicucci, E., Gaschler, K. & Ward, J. M. (1999) *Plant Biol.* **1,** 524–528.
20. Kawasaki, T., Henmi, K., Ono, E., Hataleuama, S., Iwano, M., Satoh, H. & Shimamoto, K. (1999) *Proc. Natl. Acad. Sci. USA* **96,** 10922–10926.
21. Dangl, J. D. & Jones, J. D. G. (2000) *Nature (London)* **411,** 826–833.
22. Bolwell, G. P., Davies, D. R., Gerrish, C., Auh, C.-K. & Murphy, T. M. (1999) *Plant Physiol.* **116,** 1379–1385.
23. Zhou, F., Zhang, Z., Gregersen, P. L., Mikkelsen, J. D., de Neergaard, E., Collinge, D. B. & Thordal-Christensen, H. (1998) *Plant Physiol.* **117,** 33–41.
24. Tissier, A. F., Marillonnet, S., Klimyuk, V., Patel, K., Torres, M. A., Murphy, G. & Jones, S. D. G. (1999) *Plant Cell* **11,** 1841–1852.
25. Debener, T., Lehnackers, H., Arnold, M. & Dangl, J. L. (1991) *Plant J.* **1,** 289–302.
26. Dangl, J. L., Holub, E. B., Debener, T., Lehnackers, H., Ritter, C. & Crute, I. R. (1992) in *Methods in Arabidopsis Research*, eds. Koncz, C., Chua, N.-H. & Schell, J. (World Scientific, London), pp. 393–418.
27. Koch, E. & Slusarenko, A. J. (1990) *Plant Cell* **2,** 437–445.
28. Dellagi, A., Brisset, M. N., Paulin, J. P. & Expert, D. (1998) *Mol. Plant–Microbe Interact.* **11,** 734–742.
29. Thordal-Christensen, H., Zhang, Z., Wei, Y. & Collinge, D. B. (1997) *Plant J.* **11,** 1187–1194.
30. Grant, M., Brown, I., Adams, S., Knight, M., Ainslie, A. & Mansfield, J. (2000) *Plant J.* **24,** 441–450.
31. Scheel, D. (1998) *Curr. Opin. Plant Biol.* **1,** 305–310.
32. Holub, E. B., Beynon, J. L. & Crute, I. R. (1994) *Mol. Plant–Microbe Interact.* **7,** 223–239.
33. Jabs, T., Colling, C., Tschöpe, M., Hahlbrock, K. & Scheel, D. (1997) *Proc. Natl. Acad. Sci. USA* **94,** 4800–4805.
34. Glazener, J. A., Orlandi, E. W. & Baker, C. J. (1996) *Plant Physiol.* **110,** 759–763.
35. Sagi, M. & Fluhr, R. (2001) *Plant Physiol.* **126,** 1281–1290.
36. Bolwell, G. P., Butt, V. S., Davies, D. R. & Zimmerlin, A. (1995) *Free Radical Res.* **23,** 517–532.
37. Jabs, T., Dietrich, R. A. & Dangl, J. L. (1996) *Science* **273,** 1853–1856.
38. Delledonne, M., Zeier, J., Marocco, A. & Lamb, C. (2001) *Proc. Natl. Acad. Sci. USA* **98,** 13454–13459. (First Published October 23, 2001; 10.1073/pnas.231118298)
39. Kliebenstein, D. J., Dietrich, R. A., Martin, A. C., Last, R. L. & Dangl, J. L. (1999) *Mol. Plant–Microbe Interact.* **12,** 1022–1026.
40. Rice-Evans, C., Halliwell, B. & Lunt, G. G. (1995) *Free Radicals and Oxidative Stress: Environment, Drugs and Food Additives* (The Biochemical Society, London).
41. Yu, I.-C., Parker, J. & Bent, A. F. (1998) *Proc. Natl. Acad. Sci. USA* **95,** 7819–7824.
42. Ryals, J. L., Neuenschwander, U. H., Willits, M. C., Molina, A., Steiner, H.-Y. & Hunt, M. D. (1996) *Plant Cell* **8,** 1809–1819.
43. Gaffney, T., Friedrich, L., Vernooij, B., Negrotto, D., Nye, G., Uknes, S., Ward, E. & Ryals, J. (1993) *Science* **261,** 754–756.
44. Bi, Y.-M., Kenton, P., Mur, L., Darby, R. & Draper, J. (1995) *Plant J.* **8,** 235–246.
45. Vernooij, B., Friedrich, L., Morse, A., Reist, R., Kolditz-Jawhar, R., Ward, E., Uknes, S., Kessmann, H. & Ryals, J. (1994) *Plant Cell* **6,** 959–965.
46. Pallas, J. A., Paiva, N. L., Lamb, C. J. & Dixon, R. A. (1996) *Plant J.* **10,** 281–294.
47. Draper, J. (1997) *Trends Plant Sci.* **2,** 162–165.
48. Chamnongpol, S., Willekens, H., Moeder, W., Langebartels, C., Sanderman, H. J., Van Montagu, M., Inze, D. & Van Camp, W. (1998) *Proc. Natl. Acad. Sci. USA* **95,** 5818–5823.
49. Dorey, S., Kopp, M., Geoffroy, P., Fritig, B. & Kauffmann, S. (1999) *Plant Physiol.* **121,** 163–173.
50. Freialdenhoven, A., Scherag, B., Hollricher, K., Collinge, D., Christensen, H.-T. & Schulze-Lefert, P. (1994) *Plant Cell* **6,** 983–994.
51. Bendahmane, A., Kanyuka, K. & Baulcombe, D. C. (1999) *Plant Cell* **11,** 781–791.
52. Groves, J. T. (1999) *Curr. Opin. Chem. Biol.* **3,** 226–235.
53. Beligni, M. V. & Lamattina, L. (1999) *Nitric Oxide* **3,** 199–208.